Bose-Glass–Vortex-Glass Phase Transition and Dynamic Scaling for High-T_c $Nd_{2-x}Ce_xCuO_4$ Thin Films

Satoshi Tanda, Shigeki Ohzeki, and Tsuneyoshi Nakayama
Department of Applied Physics, Hokkaido University, Sapporo 060, Japan
(Received 21 April 1992)

This paper reports the measurements of resistivities near the superconductor-insulator transition for high-T_c oxide superconductor $Nd_{2-x}Ce_xCuO_4$ single-crystal thin films. The transition was tuned by magnetic fields and/or introducing disorder. The results of the resistivities are analyzed in line with dynamical scaling theory. The product of the dynamical exponent (z_B) and the exponent for the correlation length (ν_B) is extracted. This value is consistent with that expected by the scaling theory. Our results provide the first evidence of the Bose-glass–vortex-glass phase transition in high-T_c $Nd_{2-x}Ce_xCuO_4$ single-crystal thin films.

PACS numbers: 74.65.+n, 74.70.Mq, 74.75.+t

Recently two-dimensional (2D) disordered Bose systems have attracted considerable interest in connection with the superconductor-insulator (SI) transition. It has been claimed experimentally [1–5] that the systematic introduction of disorder gives rise to the SI transition and the transition provides the universal critical sheet resistance $R_\square$ near the value of $h/(2e)^2 \approx 6.45$ kΩ. This subject has been developed as a new frontier in condensed-matter physics in which novel and fundamental physical phenomena occur. In particular, the occurrence of a new type of phase transition near the superconductor-insulator transition [6–10] is the focus of recent attention. The scaling theories [11–14] have played a key role in understanding or predicting the new phenomena. The present authors have investigated experimentally the disorder-induced SI transition in the case of high-T_c superconductor $Nd_{2-x}Ce_xCuO_4$ single-crystal thin films [5]. The use of high-T_c $Nd_{2-x}Ce_xCuO_4$ thin films has an advantage for our purpose, i.e., the measurements are made by varying gradually the oxygen contamination in *single-crystal* thin films by heat treatment without changing film thickness. This has made it possible to investigate systematically the disorder-induced SI transition for high-T_c thin films.

The magnetic field can also probe the details of the SI transition. This Letter reports the experimental results on the magnetic-field-induced SI transition using high-T_c oxide superconductor $Nd_{2-x}Ce_xCuO_4$ single-crystal thin films. We have measured the temperature and magnetic-field dependence of the resistivity of $Nd_{2-x}Ce_xCuO_4$ single-crystal thin films, which were prepared by the molecular-beam-epitaxy (MBE) method. The experimental results are analyzed with the dynamic scaling theory proposed recently [12]. We show that the good scaling occurs when the resistivities are plotted as a function of the scaling variable $[c_0(B-B_c)/T^{1/z_B\nu_B}]$ near the SI transition for our samples. The magnetic-field-induced transition is continuous and the critical sheet magnetoresistance is estimated to be close to $R_\square^* = 8.5$ kΩ. It should be also emphasized that the current-voltage characteristics are Ohmic, which is in accord with the theoretical prediction [12] that the new metallic state exists in the middle of the SI transition. The dynamical exponent ($\Omega_B \simeq |B-B_c|^{z_B\nu_B}$ where Ω_B is a characteristic frequency), introduced in the scaling theory, was obtained to be $z_B\nu_B = 1.2 \pm 0.1$.

It is well known that the high-T_c oxide superconductor $Nd_{2-x}Ce_xCuO_4$ is peculiar among copper-based oxide superconductors with perovskite structures [15]. The ordinary copper-oxide high-T_c superconductors have CuO networks with pyramid or octahedra type arrangements, and, in addition, charge carriers in the normal state are holes. While the $Nd_{2-x}Ce_xCuO_4$ system consists of two-dimensional (2D) CuO_2 layers with no apical oxygen, the CuO_2 layers form an ideal 2D conducting sheet as verified by the observations that the normal-state transport properties of the single-crystal films show the typical characteristics of weak localization associated with two dimensionality [5,16–18].

$Nd_{2-x}Ce_xCuO_4$ single-crystal films were grown on a $SrTiO_3$ (100) single crystal by the method of MBE using Knudsen cell sources for Nd, Cu, and Ce. After deposition, the oxygen flow to the film surface was stopped immediately and the substrate was cooled from 800 °C to room temperature in the background pressure of 10^{-4} Torr. The appearance of only (002n) peaks indicates that the (001) plane is highly oriented parallel to the film surface. In order to obtain thoroughly oxidized samples, the films were heated up to 950 °C in air and kept at that temperature for 2 h. These oxidized films were reduced in the background of Ar pressure of 0.4 Torr ranging from 450 to 750 °C for 20 min. This reduction in the vacuum ambient plays a role in reducing the oxygen concentration in $Nd_{2-x}Ce_xCuO_4$ films, which is required for the appearance of the superconductivity. The film thickness, determined from a cross section of the films by the electron microscope, was 1000 Å within an accuracy of a few percent. The temperature dependence of the resistivity $\rho(T)$ was measured by the standard four-terminal method with evaporated gold electrodes. The current terminals were covered with gold along the edge of the films in order to eliminate the ambiguity due to inhomogeneous

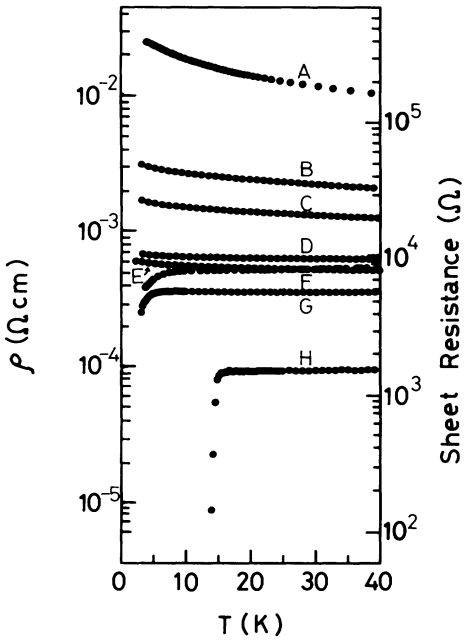

FIG. 1. Temperature dependence of resistivities (left-hand scale) for $Nd_{2-x}Ce_xCuO_4$ single-crystal films at various stages of disorder controlled by annealing process. Curves A-G are for $x=0.18$, and H is for $x=0.16$. The annealing conditions were A at 450 °C, B at 500 °C, C at 550 °C, D at 600 °C, E at 650 °C, F at 700 °C, G at 750 °C, and H at 750 °C for 20 min in a vacuum ambient. The right-hand scale refers to the sheet resistance per CuO_2 layer (see text).

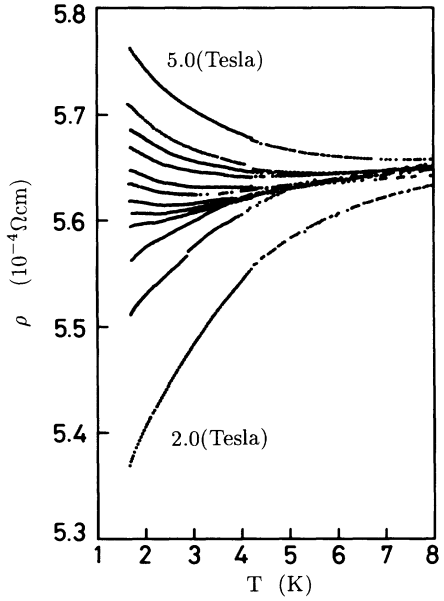

FIG. 2. Temperature dependence of resistivities for line F in Fig. 1 in magnetic fields ranging from 2.0 to 5.0 T. The magnetic fields are 2.0, 2.4, 2.6, 2.8, 2.9, 3.0, 3.1, 3.2, 3.4, 3.6, 4.0, and 5.0 T in order of increasing resistivity. The magnetic fields are applied perpendicularly to the film surface.

current flow arising from strong anisotropy. The current density was 10 A/cm^2 throughout our measurement. The temperature dependence of the resistivity, $\rho(T)$, for the $Nd_{2-x}Ce_xCuO_4$ film at various stages of oxygen reduction is shown in Fig. 1.

The residual resistivity was 75 $\mu\Omega$ cm for sample H ($x=0.16$). This value is small compared with those of bulk single crystals [17,19]. This is due to the fact that it is easier to reduce oxygen impurities in films than in bulk samples. These vacuum-annealed films, with optimum reduction, are characterized by a sharp superconducting transition with $T_c(\rho=0)=15$ K and a transition width of less than 0.9 K. It should be emphasized that the data of sample H ($k_Fl=20$ at $T=18$ K) agree fairly well with the theory by Aslamazov and Larkin [20], indicating that 2D fluctuations are relevant for this less disordered sample [21].

The magnetic field was applied perpendicularly to the film surface for sample F in Fig. 1. The resistivity was measured as a function of temperature in detail in the vicinity of magnetic fields inducing the SI transition. Figure 2 shows the observed resistivity of sample F ($k_Fl=2.2$ at $T=18$ K) as a function of temperature under magnetic fields ranging from 2.0 to 5.0 T. We see, from the data of Fig. 2, that superconductivity is appreciably suppressed by applying magnetic fields and approaches the insulating phase continuously. The scaling theory [12] predicts that resistivity scales as

$$\rho(B,T)=\frac{h}{4e^2}f\left[\frac{c_0(B-B_c)}{T^{1/z_B\nu_B}}\right], \tag{1}$$

under magnetic field B, where c_0 is a nonuniversal constant and B_c is the critical magnetic field characterizing the SI transition. z_B and ν_B are the dynamical critical exponent and the static critical exponent for superconducting correlation length ξ_B, respectively. The definitions are given by $\xi_B\sim(B-B_c)^{-\nu_B}$ and $\Omega_B\sim\xi_B^{-z_B}$ where Ω_B is a characteristic frequency. Near the transition, one expects a diverging length ξ_B, which sets the length scale characterizing the system. By increasing magnetic fields, a remarkable possibility arises, namely, vortices should be delocalized and undergo a Bose condensation at some critical field B_c [12]. This condensation also requires the appearance of the Bose glass phase (paired electrons are localized).

Now let us analyze our experimental data using the scaling form of Eq. (1). First, we determine the critical magnetic field B_c, where vortices undergo a Bose condensation. By differentiating the data given in Fig. 2 with respect to temperature, we have obtained, from the condition $(d\rho/dT)_{1.7\,K}=0$, the value of $B_c=2.9$ T. This critical magnetic field B_c is given by the arrow in Fig. 3. This transition yields the critical sheet magnetoresistance of $R_\square^*\simeq 8.5$ kΩ. This value was estimated by extrapolating the resistance at $(d\rho/dT)_{B=B_c}=0$ at the lowest tempera-

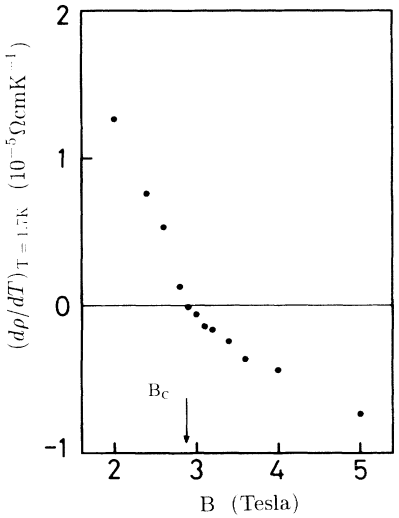

FIG. 3. Values of the slopes $(d\rho/dT)_{T=1.7\,\mathrm{K}}$ are plotted as a function of magnetic field. The critical magnetic field $B_c=2.9$ T is determined from the point where the slope becomes zero.

ture. Note that the sheet resistance $R_{\square}^{*}$ per CuO_2 layer was obtained using the relation $R_{\square}^{*}=\rho/d$, where d ($=6.03$ Å) is the lattice spacing between CuO_2 layers. This relation is reasonable from the confirmation of 2D weak localization for our sample [5]. Second, in order to determine the value of the critical exponent $z_B\nu_B$ from experimental data, we use the differential form of the scaling function of Eq. (1), which is given by

$$\left(\frac{d\rho}{dB}\right)_{B=B_c}=\frac{c_0 h}{4e^2}T^{-1/z_B\nu_B}f'(0)\,. \tag{2}$$

We have plotted in Fig. 4 the data for $(d\rho/dB)_{B=B_c}$ as a function of the inverse of temperature $1/T$ using logarithmic scales. The solid lines show the power law with

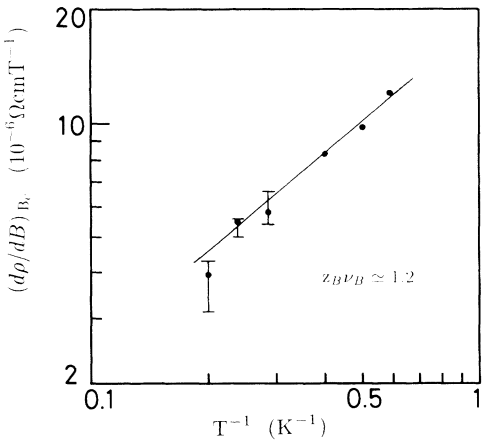

FIG. 4. Logarithmic plot of $(d\rho/dB)_{B=B_c}$ as a function of $1/T$. The product of the exponents $(z_B\nu_B)$ is extracted as $z_B\nu_B=1.2\pm0.1$ from the slope.

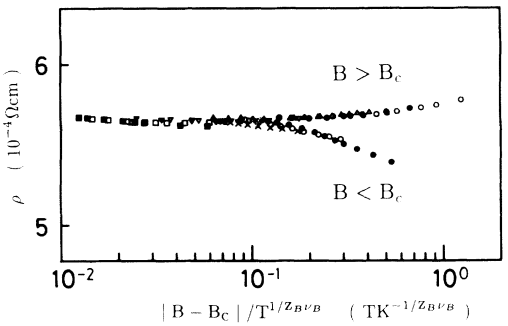

FIG. 5. Scaling dependence of the resistivities as a function of the scaling variable $[c_0(B-B_c)/T^{1/z_B\nu_B}]$ where the values $B_c=2.9$ T and $z_B\nu_B=1.2$ are used. The symbols correspond to various applied magnetic fields given in Fig. 2.

$z_B\nu_B\simeq 1.2\pm0.1$. It should be emphasized that this value is consistent with the predicted theoretical constraint $z_B\nu_B\geq 1$.

Figure 5 shows the scaling dependence of the resistivities as a function of the scaling variable $[c_0(B-B_c)/T^{1/z_B\nu_B}]$ using the value for the critical magnetic field $B_c=2.9$ T and the exponent $z_B\nu_B=1.2$. The data in Fig. 5 represent the resistivities $\rho(T,B)$ as a function of scaling variable $[c_0(B-B_c)/T^{1/z_B\nu_B}]$. It can clearly be seen that all of the data fall on one of two universal curves. All resistivities in the insulating side (upper curve in Fig. 5) have the form of the conductance $\exp[-(T_0/T)^{1/2}]$, indicating that the variable-range hopping is a dominant process for the transport [22]. This form is in fairly good agreement with the prediction by Fisher [12]. We plot in Fig. 6 the characteristic temperature T_0 as a function of $B-B_c$ on a logarithmic scale. The plotted data show

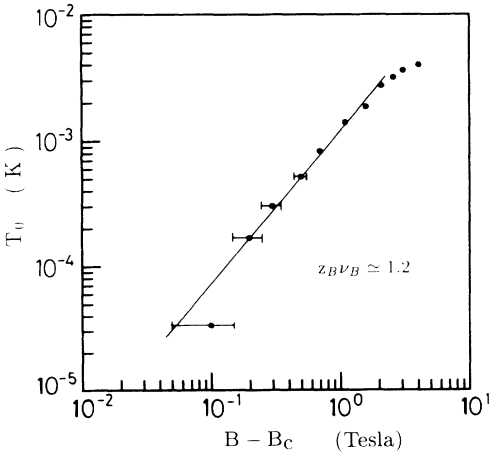

FIG. 6. The characteristic temperature T_0 as a function of $B-B_c$ on a logarithmic scale. The exponent $z_B\nu_B$ is found to be 1.2 ± 0.1 from the relation $T_0\propto(B-B_c)^{z_B\nu_B}$. In the regime $B>5$ T, $z_B\nu_B$ is close to the mean-field value of 0.5. We have determined the exponent in the critical regime.

clearly the power law and we have the relation $T_0 \propto (B-B_c)^{z_B\nu_B}$ with $z_B\nu_B = 1.2 \pm 0.1$. It is remarkable that this estimated value agrees well with the value $z_B\nu_B = 1.2 \pm 0.1$ obtained from the analysis from the data given in Fig. 4. This agreement indicates the consistency of our analysis based on the dynamic scaling theory [12]. To summarize, we have reported the first observation of the field-induced SI transition *for* high-T_c material. Observed resistivities near the field-tuned SI transition provide the evidence of the Bose-glass–vortex-glass phase transition as well as the validity of the dynamic scaling theory describing this transition.

The authors would like to thank Dr. A. Ohi for useful discussions. We thank K. Takahashi and M. Honma for experimental support. We are also grateful to T. Sambongi and K. Yamaya, who assisted us with the use of high-magnetic-field facilities. Hiroshi Takahashi of Eiko Engineering Company is thanked for his support. This work was supported in part by a Grant-in-Aid of the Japan Ministry of Education, Science and Culture.

[1] B. G. Orr, H. M. Jaeger, and A. M. Goldman, Phys. Rev. B **32**, 7586 (1985); B. G. Orr *et al.*, Phys. Rev. Lett. **56**, 378 (1986); H. M. Jaeger *et al.*, Phys. Rev. B **40**, 182 (1989).

[2] S. Kobayashi and F. Komori, J. Phys. Soc. Jpn. **57**, 1884 (1988); S. Kobayashi *et al.*, J. Phys. Soc. Jpn. **59**, 4219 (1990).

[3] D. B. Haviland, Y. Liu, and A. M. Goldman, Phys. Rev. Lett. **62**, 2180 (1989); D. B. Haviland *et al.*, Physica (Amsterdam) **165&166B**, 1457 (1990).

[4] S. J. Lee and J. B. Ketterson, Phys. Rev. Lett. **64**, 3078 (1990).

[5] S. Tanda, M. Honma, and T. Nakayama, Phys. Rev. B **43**, 8725 (1991); S. Tanda *et al.*, Physica (Amsterdam) **185–189C**, 1323 (1991).

[6] R. H. Koch *et al.*, Phys. Rev. Lett. **63**, 1511 (1989).

[7] A. F. Hebard and M. A. Paalanen, Phys. Rev. Lett. **65**, 927 (1990).

[8] T. K. Worthington *et al.*, Phys. Rev. B **43**, 10538 (1991).

[9] P. L. Gammel, L. F. Schneemeyer, and D. J. Bishop, Phys. Rev. Lett. **66**, 953 (1991).

[10] Y. Liu *et al.*, Phys. Rev. Lett. **67**, 2068 (1991).

[11] M. P. A. Fisher, Phys. Rev. Lett. **62**, 1415 (1989); D. S. Fisher, M. P. A. Fisher, and D. A. Huse, Phys. Rev. B **43**, 130 (1991).

[12] M. P. A. Fisher, Phys. Rev. Lett. **65**, 923 (1990); A. T. Dorsey and M. P. A. Fisher, Phys. Rev. Lett. **68**, 694 (1992).

[13] M-C. Cha, M. P. A. Fisher, S. M. Girvin, M. Wallin, and A. P. Young, Phys. Rev. B **44**, 6883 (1991).

[14] X. G. Wen and A. Zee, Phys. Rev. Lett. **62**, 1937 (1989); X. G. Wen and A. Zee, Int. J. Mod. Phys. B **4**, 437 (1990).

[15] Y. Tokura, H. Takagi, and S. Uchida, Nature (London) **337**, 345 (1989).

[16] A. Kussmaul, J. S. Moodera, P. M. Tedrow, and A. Gupta, Physica (Amsterdam) **177C**, 415 (1991).

[17] S. J. Hagen, X. Q. Xu, W. Jiang, J. L. Peng, Z. Y. Li, and R. L. Greene, Phys. Rev. B **45**, 515 (1992).

[18] Y. Hidaka *et al.*, J. Phys. Soc. Jpn. **60**, 1185 (1991).

[19] Z. Z. Wang, T. R. Chien, N. P. Ong, J. M. Tarascon, and E. Wang, Phys. Rev. B **43**, 3020 (1991); Y. Hidaka and M. Suzuki, Nature (London) **338**, 635 (1989).

[20] L. G. Aslamazov and A. I. Larkin, Phys. Lett. **26A**, 238 (1968); A. G. Aronov, S. Hikami, and A. I. Larkin, Phys. Rev. Lett. **62**, 965 (1989).

[21] We have tried to fit the experimental data of lines *F* and *H* in Fig. 1 by the Aslamazov-Larkin [20] and the Maki-Thompson theory [K. Maki, Prog. Theor. Phys. **39**, 897 (1968); R. S. Thompson, Phys. Rev. B **1**, 327 (1970)]. Though line *H* ($k_Fl = 19$) was fitted fairly well by these theories, sample *F* ($k_Fl = 2.2$) was not in magnetic fields ranging from 0 to 2.9 T. This indicates that sample *F* has heavily disordered characters compared with sample *H*.

[22] The details on hopping behavior of the insulating side of Fig. 5 will be published elsewhere. It should also be mentioned that samples *D* and *E* show clearly the characteristic behavior of hopping conduction as reported by S. Tanda *et al.*, Physica (Amsterdam) **185–189C**, 1323 (1991).